Received July 28, 2019, accepted August 21, 2019, date of publication August 26, 2019, date of current version September 6, 2019.

Digital Object Identifier 10.1109/ACCESS.2019.2937385

Isolation Enhancement for 1 × 3 Closely Spaced E-Plane Patch Antenna Array Using Defect Ground Structure and Metal-Vias

ZICHENG NIU[1], HOU ZHANG[1], QIANG CHEN[2], AND TAO ZHONG[1]
[1]Air-Defense and Antimissile Institute, Air Force Engineering University, Xi'an 710051, China
[2]Air Force Early Warning Academy, Wuhan 430019, China

Corresponding author: Zicheng Niu (nzc585@126.com)

ABSTRACT This paper introduces an effective solution for improving isolation in linear antenna array. The array is composed of three-element E-plane single feed patch antennas (the overall size is 0.59 λ_0 × 1.02 λ_0), which are closely placed with approximately 0.037 λ_0, where λ_0 is the free-space wavelength at 4 GHz. The decoupling structure consists of T-shaped and rectangular ring shaped defect ground structure (DGS) with six metal-vias. The decoupling mechanism is illustrated by investigating the current vector on the ground plane. The current distribution indicates that the decoupling structure along the outer edge of the radiation patch sever as coupling current converter to produce reverse current opposite to the direction of the ground coupling current, which transmits along the outer edge of the radiation edge. The measured results show that the enhancement in the isolation at 4 GHz is 10.8 dB for |S21|, 17.5 dB for |S23| and 16.6 dB for |S31|. After applying the decoupling structure, the 10-dB impedance bandwidth (3.95 - 4.04 GHz) of antenna 1 remains unchanged. Meanwhile, the 10-dB impedance bandwidth of the antenna, which is located in the middle of the three-element antenna array, increases by 86 MHz (from 114 MHz to 200 MHz). When the decoupling structure is loaded, the maximum gain only decreases by 0.12 dB (from 3.94 to 3.82 dB). The decoupling structure has the advantages of simple structure, easy processing, and independent design of the array, so it can be applied to multielement patch array, such as massive multiple-input multiple-output (M-MIMO) system.

INDEX TERMS Linear antenna array, defect ground structure (DGS), mutual coupling, isolation.

I. INTRODUCTION

With the development of multi-antenna system [1]–[3], electromagnetic wave interference between antennas has become one of the most concerned problems in array antenna design. The mutual coupling can bring about many undesirable results, such as deteriorative matching, disturbed radiation pattern and so on [4]. Usually, mutual coupling can be ignored when the center-to-center distance between adjacent antennas is kept over $\lambda_0/2$ (λ_0 is the free space wavelength of center frequency). However, in practical applications, antenna elements need to be tightly placed to adapt the limited space for array. Therefore, it is necessary to decouple the compact multi-antenna system.

In the previous studies, there have been many reports on the decoupling method of 1 × 2 linear antenna array, such as metasurface [5]–[6], polarization-conversion isolator [7], electromagnetic bandgap (EBG) [8]–[11] and resonators [12], [13] and the like. Papers [5], [6] use the metasurface to create a negative permeability to attenuate the coupling waves in space. Despite achieving high isolation, it destroys the antenna matching and requires high profile. In [11], the EBG structure is placed between two microstrip antennas to suppress transmission of higher order modes. Since the periodic structure is etched between the antennas, the spacing between the antennas becomes large, which destroys the compactness of the array. Paper [13] presents the implementation of a pair of parallel coupled-line resonators (PCR) for decoupling in two-element antennas array. The PCR provides higher order rejection that enhances the bandstop characteristics to improve isolation. Like EBG structure, although the better isolation is achieved in the 1 × 2 linear antenna array, it increases the overall size due to being loaded in the middle of the antennas. Neutralization lines [14]–[17] can use metallic slit to transmit electromagnetic waves from one antenna to another. Therefore, it can create an opposite current between antennas to reduce mutual coupling at certain frequencies. However, there is no

The associate editor coordinating the review of this article and approving it for publication was Yanhui Liu.

general method for the size and connection position of the neutralization line, so the simulation software can only be used for tuning and optimization of the neutralization line and antenna, which increases the design time and difficulty. In [18]–[20], the decoupling network is added to feed port of antenna to reduce mutual coupling. The decoupling principle of the decoupling network is to use the partial coupling current near the excited antenna and the current without decoupling network to cancel each other to improve the isolation. For the microstrip decoupling network, the size of the decoupling network is relatively large when the antenna is working in the low-frequency band, which is not conducive to the miniaturization of the array. The lumped element is used to replace the microstrip line, which greatly reduces the size of the network. However, the lumped element not only has high Q value, which makes the network debugging difficult, but also reduces the radiation efficiency of the antenna.

However, the abovementioned decoupling structure only applies to the decoupling of two-element antennas. In the past few years, several studies [21]–[25] have been carried out on the enhancement of the isolation of the linear multi-element antenna array. In [22], the array antenna decoupling surface (ADS) is loaded above the 1 × 8 antenna array. The partially diffracted waves from the ADS can be controlled to cancel the unwanted coupled waves. Nevertheless, the ADS needs to be at least $\lambda_0/4$ away from the array, which inevitably increases the profile. And above all, although the mutual coupling between adjacent antennas is suppressed, coupling between non-adjacent antennas still exists. Paper [23] proposed a graphene-based frequency selective surface (FSS) to reduce the coupling effects in 1 × 4 antenna arrays. However, this method not only requires high profile, but also sophisticated installation technique to fix FSS between antennas in practical application. In [25], an efficient decoupling network is proposed to decouple closely spaced multielement antenna array. As the decoupling network needs to be combined with the antenna array design, it adds to the difficulty of design work.

The traditional loading method of defect ground structure (DGS) is etching the structure in the middle of the antennas to form a bandstop filter, which blocks the propagation of coupling current on the ground. However, the conventional method undoubtedly increases the spacing between the antennas. In order to obtain high isolation in the closely spaced three-element antenna array, the DGS is etched along the outer edge of the radiation patch, which generates the current opposite to the coupling current to undermine the mutual coupling.

In this paper, the authors propose a decoupling structure, consisting of T-shaped and rectangular ring DGS with six metal-vias. It is worth to mention that it is the first time to propose an approach of using DGS etched along the outer edge of the radiation patch to improve isolation in three-element closely packed antenna array. The proposed decoupling structure has the following attractive features.

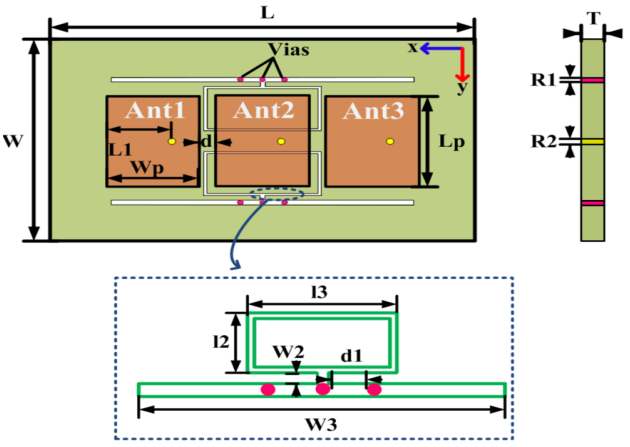

FIGURE 1. Proposed decoupling structure for the three-element antenna array.

TABLE 1. Dimension of the antenna array.

Symbol	Value (Units: mm)	Symbol	Value (Units: mm)
W	44	l3	21.2
L	76.6	W2	1
W_P	17	W3	54.8
L_p	20	d1	3
L1	3.3	R1	0.5
d	2.8	R2	0.6
l2	9.7	T	1.6

1) It can be applied to closely spaced linear antenna array. In this paper, the decoupling structure is applied to three-element antennas with edge-to-edge distance of 0.037 λ_0, which is smaller than all that of previous studies using DGS [26]–[29].
2) It is proved that the mutual coupling of the array is less −20 dB within the 10-dB impedance bandwidth of the antenna, demonstrating the potential for a wide band decoupling.
3) It increases the bandwidth of the antenna 2. The rectangular ring structure is etched below antenna 2 to introduce capacitive reactance, which offends the inductive reactance introduced by the coaxial and improves the bandwidth of antenna 2.
4) It has the advantage of simple structure, low profile, easy processing, and independent design of antenna array

II. THE THREE-ELEMENT ANTENNA ARRAY DESIGN AND ANALYSIS

The proposed three-element antenna array with decoupling structure is shown in Fig.1. Design and development of the proposed three-element antennas with decoupling structure has been carried out by using parameters analysis and optimization in HFSS 13.0.

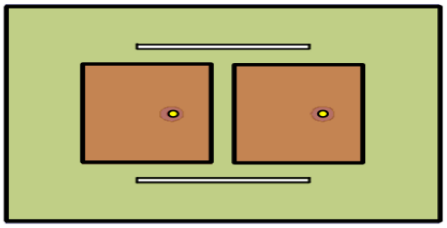

FIGURE 2. The two-element antenna array with rectangular DGS.

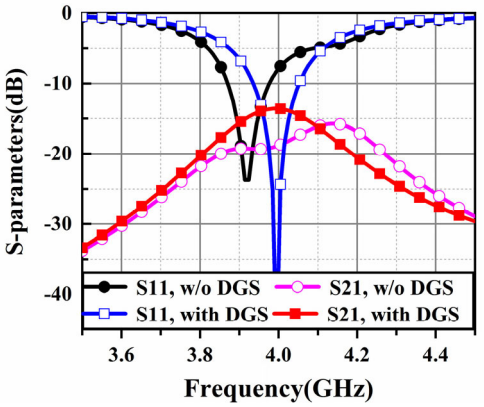

FIGURE 3. Simulated S-parameters of the two-element antenna array with and without rectangular DGS.

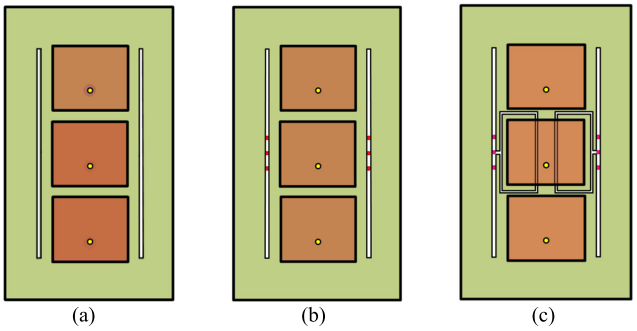

FIGURE 4. Evolution of the decoupling structure. (a) Stage1: Rectangular DGS. (b) Stage 2: Rectangular DGS with six metal-vias. (c) Proposed decoupling structure: T-shaped and rectangular ring DGS with metal six metal-vias.

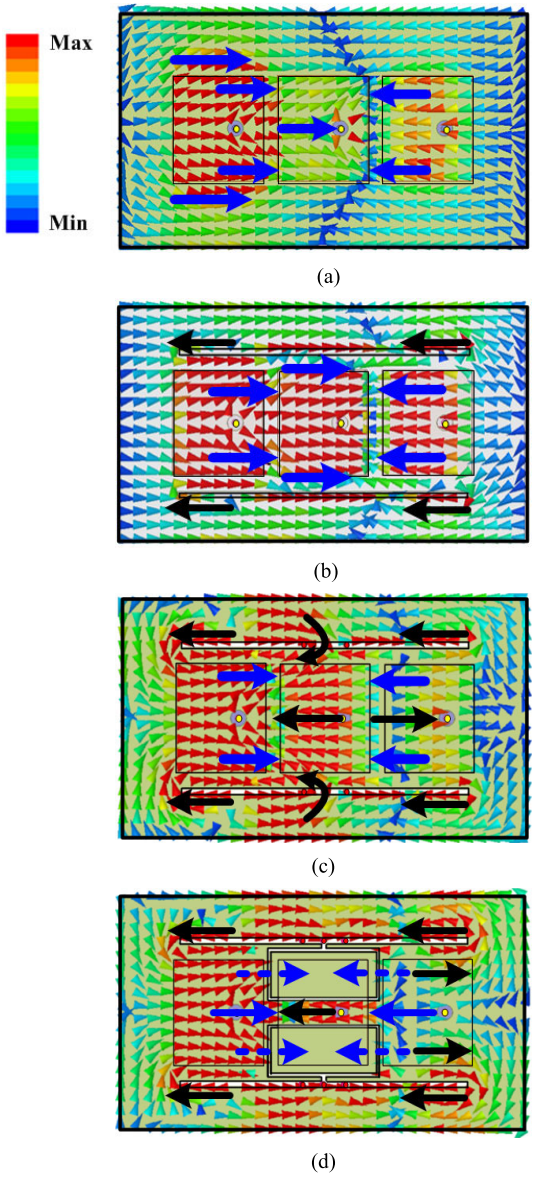

FIGURE 5. Current distribution on the ground plane at 4 GHz. (a) Original antenna array. (b) Stage 1. (c) Stage 2. (d) Proposed decoupling structure. Blue arrows show the coupling current. Black arrows represent the reverse current. Blue dash lines show the diminished coupling current and black dash lines represents the diminished reverse current.

A. THREE-ELEMENT ARRAY WITH DECOUPLNIG STRUCTURE DESIGN

The decoupling structure consists of a pair of T-shaped and rectangular ring DGS with six metal-vias. The three probe-fed patches operate at 4 GHz with a common dielectric and ground plane. When a dielectric substrate with high dielectric constant is applied, since surface waves are more easily excited along E-plane, the mutual coupling of E-plane is stronger than that H-plane. Therefore, a three-element E-plane antenna array printed on a substrate with high dielectric constant is designed to demonstrate the ability of the decoupling structure. The substrate employs FR4 with relative permittivity of 4.4 and loss tangent of 0.02. The edge-to-edge spacing of antennas is maintained at 2.8 mm (0.037 λ_0, where λ_0 is the free-space wavelength at 4 GHz). TABLE 1 shows the detail dimensions of the three-element antenna array with the decoupling structure.

Firstly, the authors design a rectangular DGS to block the propagation of the coupling current on the ground in the closely spaced two-element microstrip antenna array [30], as shown in Fig.2. It can be seen from Fig.3 that after loading the rectangular DGS, the isolation increases from 13.6 to 18.7 dB at 4 GHz, but the center frequency is slightly offset (from 4 GHz to 3.92 GHz). After loading the rectangular DGS, the 10-dB impedance bandwidth of the antenna is not affected and is still 101 MHz.

The evolution of the decoupling structure is described in Fig.4. Paper [31] mentions that the DGS method for

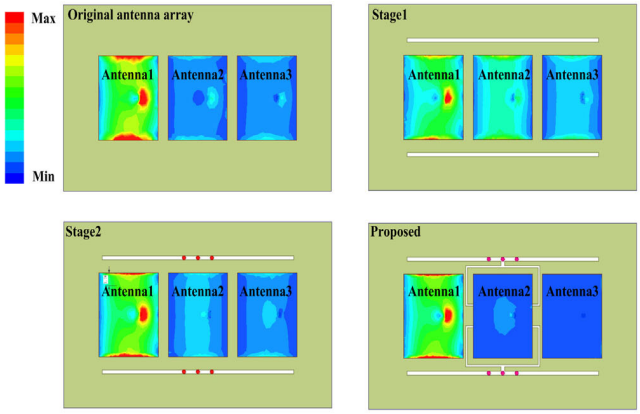

FIGURE 6. Current distribution on the patches at 4 GHz.

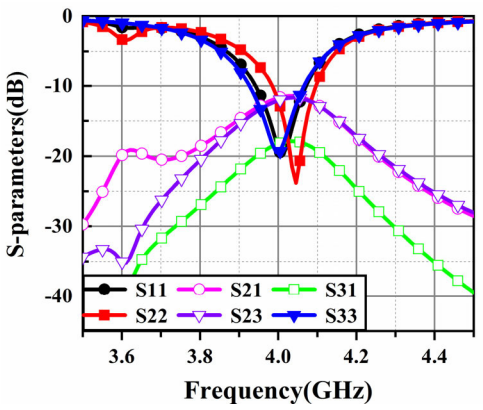

(a)

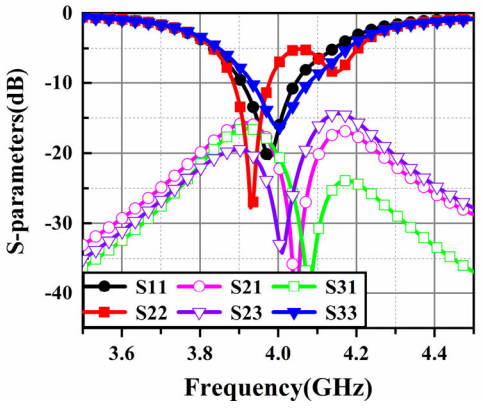

(b)

FIGURE 7. Simulated S-parameters of the three-element antenna arrays. (a) Stage 1. (b) Stage 2.

enhancing isolation is determining its shape, size and position. A properly designed DGS introduces currents opposite in direction to the original coupling currents thus reduces mutual coupling. In this paper, the proposed structure is etched on the ground plane along the radiating outer edge of the patch to reverse part of the common ground current, which counteracts the coupling current to improve the isolation. Based on the decoupling technique of two-element

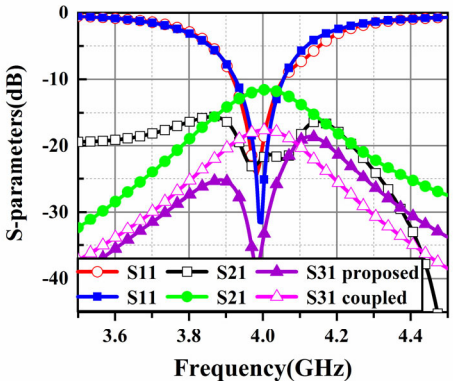

(a)

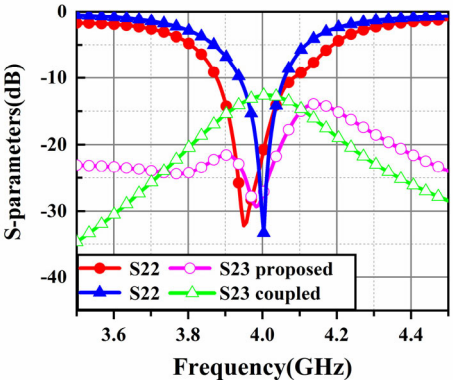

(b)

FIGURE 8. Simulated S-parameters of the three-element antenna arrays with and without the proposed decoupling structure. (a) Simulated results of port 1. (b) Simulated results of port 2.

microstrip antenna array, the length of the rectangular DGS is extended and applied to the three-element microstrip antenna array (Stage 1). However, the Stage1 cannot attenuate the coupling current of the three-element linear array due to the interaction of common ground current between non-adjacent antennas. In order to further enhance isolation, six metal-vias are added to the rectangular DGS, which is illustrated in Fig. 4 (b). Finally, the rectangular structure is transformed into T-shaped, and a pair of rectangular rings is added to improve the matching of the three-element antennas and correct the shift of the center frequency of the antenna 2 at 4 GHz.

B. DECOUPLING MECHANISM ANALYSIS

It is well known that the coupling ground surface currents have a great influence on the port-to-port isolation. In order to further study the high isolation provided by the proposed decoupling structure, the authors use the HFSS 13.0 to generate the images of the surface current vector distribution on the ground plane in Fig.5 when antenna 1 is excited and antenna 2 and 3 is terminated. Fig.5 (a) shows that the current is coupled from antenna 1 to antenna 2 and 3 along the outer side of the radiating edges and directly below the patch. As can be seen from Fig.5 (b), the rectangular DGS is etched on the ground along the outer edge of the radiation

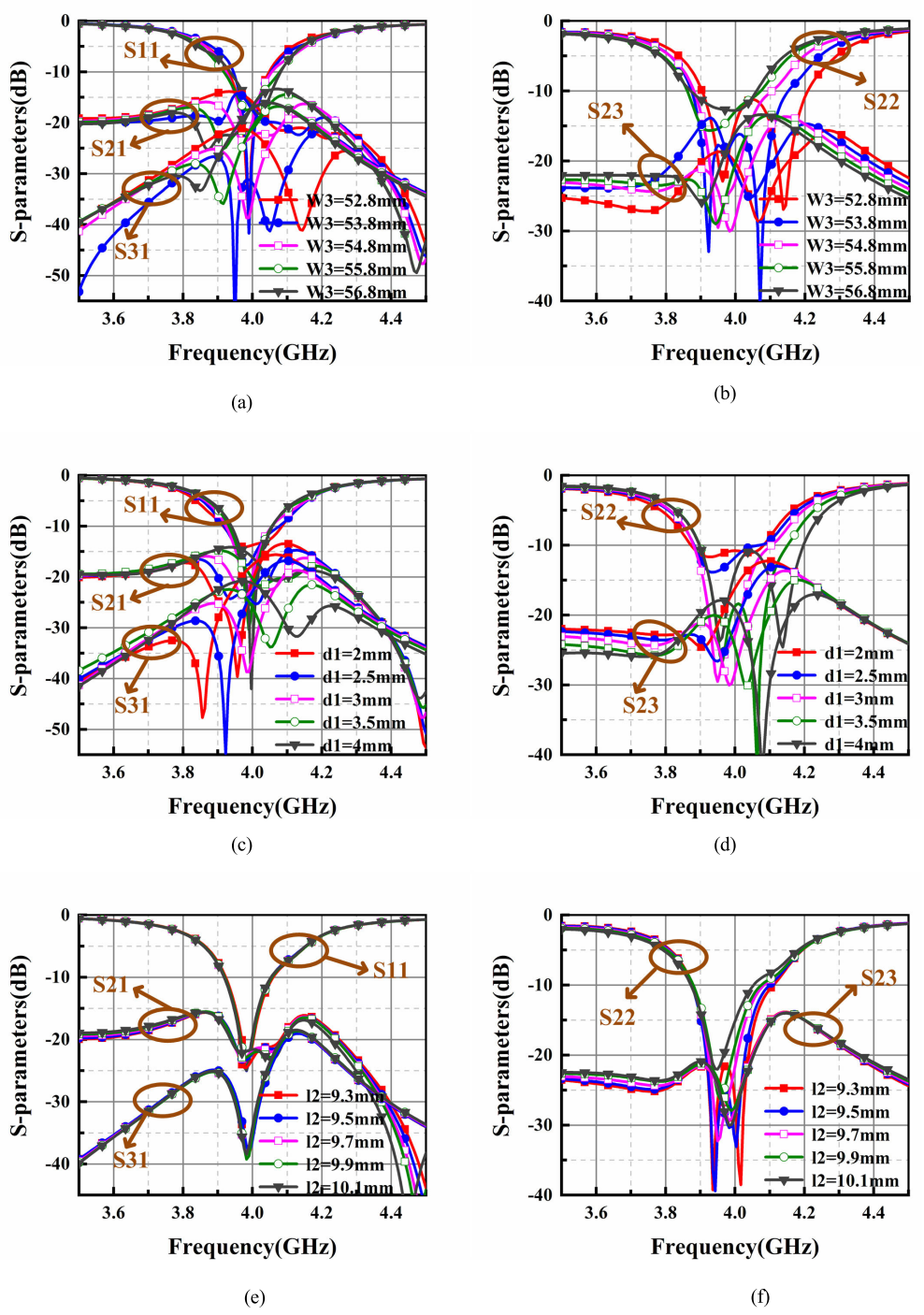

FIGURE 9. Simulated reflection and transmission coefficient characteristics of the antenna array with and without the decoupling structure for different parameters. (a) Simulated results of port 1 respect to the length of T-shaped structure - W3. (b) Simulated results of port 2 respect to the length of T-shaped structure - W3. (c) Simulated results of port 1 respect to distance between the metal vias – d1. (d) Simulated results of port 2 respect to the distance between the metal vias – d1. (e) Simulated results of port 1 respect to the width of rectangular ring – l2. (f) Simulated results of port 2 respect to the width of rectangular ring – l2.

patch, and the current opposite to the coupling current is generated at both ends of the rectangular DGS. However, unlike the two-element antenna array, the coupling between non-adjacent antennas in the three-element antenna array cannot be ignored. It can be concluded from Fig.7 (a) that the isolation of the three-element antenna array is still low after the rectangular DGS is loaded. Therefore, the method proposed in [30] to etch the rectangular DGS cannot solve the coupling of the multi-element linear arrays. In Fig.5 (c), the rectangular DGS provides the reverse current at the outer

edge of antenna 1 and antenna 3, and the metallized vias make partial coupling currents to reverse near antenna 2, alleviating the coupling current and improving isolation. However, the coupling current on the ground directly below antenna 1 and antenna 3 does not attenuate. Under the interaction of coupling and reverse current, the center frequency of antenna 2 is offset and dose not reach resonance at 4 GHz in Fig.7 (b). To improve the situation, the rectangular structure evolves into T-shaped structure and a pair of rectangular rings is added to further inhibit the interaction of the coupling current on the ground plane directly below antenna 1 and 3 with the current near the feed point of antenna 2 in Fig.5 (d). The current on the patch is shown in Fig.6. It can be seen that different decoupling structures have different effects on the current. Compared with the decoupling structure designed in other stages, the proposed decoupling structure can effectively attenuate the coupling between adjacent and non-adjacent patches when the antenna 1 is excited and antenna 2 and 3 is terminated.

III. SIMULATD RESULTS DISCUSSION

In this section, the S-parameters of the three-element antenna array with and without the decoupling structure are discussed. The dimension of the structure is analyzed by parameter scanning.

A. SIMULATED RESULTS AND DISCUSSION

The simulated reflection and transmission coefficient of the compact array with and without the decoupling structure are superposed in Fig.8. It can be noticed that after loading the decoupling structure, |S21| and |S23| (mutual coupling between adjacent antennas) are reduced by 10.1 dB and 14.5 dB respectively at 4 GHz. The isolation between non-adjacent antennas – |S31| is increased by 15.6 dB at the center frequency. Moreover, the structure does not deteriorate the matching of the antenna and the 10-dB impedance bandwidth of antenna 2 increased from 120 MHz (3.94-4.06 GHz) to 210 MHz (3.87-4.08 GHz). The reason is that grooving around the feed of antenna 2 is equivalent to introducing the capacitive reactance, which can counteract some inductive reactance introduced by coaxial feed, improve the imaginary part matching, and achieve the purpose of increasing isolation.

B. PARAMETER ANALYSIS

The parametric study results are presented in Fig.9. From Fig.9 (a) and (b), with the increase of W3, the maximum isolation of adjacent and non-adjacent antennas moves to the lower frequency, since the increase in W3 lengthens the flow path of the reverse current. Meanwhile, the matching of antenna 1 is not deteriorated, while the bandwidth and matching of antenna 2 are affected by the change of W3. From Fig.9 (c) and (d), with the increase of d1, the maximum isolation of adjacent and non-adjacent antennas moves to the upper frequency, since the current flow between the metal-vias increases toward the antenna 2 to disturb the reverse current

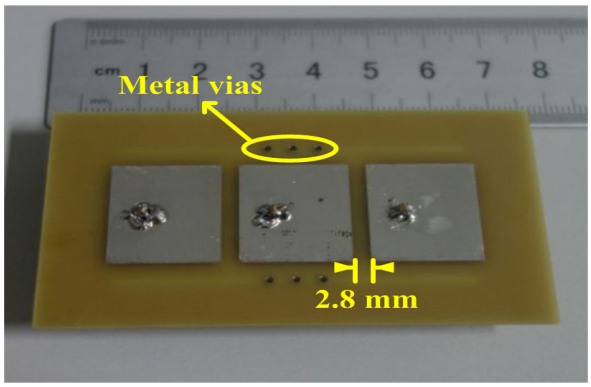

(a)

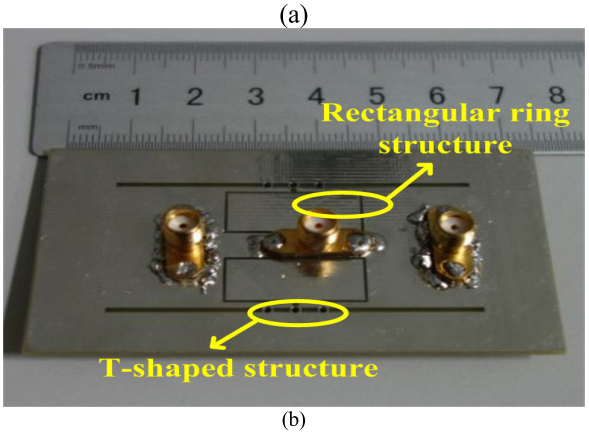

(b)

FIGURE 10. Fabricated 1 × 3 closely coupled E-plane patch antenna with decoupling structure. (a) Top view. (b) Bottom view.

distribution on the ground. At the same time, the matching of antenna 2 gradually improves with the increase of d1, reaching the local optimal at d1 = 3 mm, and then deteriorates gradually with the increase of d1. From the analysis in the previous section, it can be noticed that the function of l2 is to adjust the matching of antenna at 4 GHz, which is well demonstrated in Fig.9 (e) and (f). With the increase of l2, the other S-parameters of the antenna remain unchanged except that the impedance matching of antenna 2 becomes worse, as the width of the rectangular ring groove affects the current near the feed point of antenna 2.

IV. MEASURED RESULTS DISCUSSION

A prototype of the 1 × 3 antenna array with decoupling structure has been manufactured and tested to verify the theoretical analysis. Its photograph is shown in Fig.10. The vector network analyzer and the microwave anechoic chamber are used to measure reflection coefficients, isolation, and radiation pattern characteristics, respectively.

A. S-PARAMETERS

The measured reflection coefficients (given by |S11| and |S22|) and the transmission coefficients (given by |S21|, |S31| and |S23|) are depicted in Fig.11. The measured center frequency of the antenna 1 shifts slightly to lower frequency compared to the simulated results, which can be caused by fabrication tolerance and measurement errors. It can be

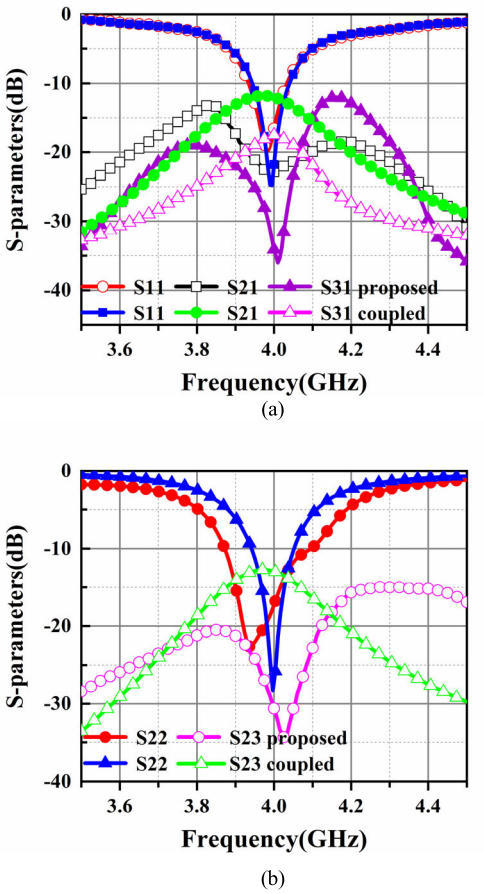

FIGURE 11. Measured S-parameters of the three-element linear antenna array with and without the proposed decoupling structure. (a) Simulated results of port 1. (b) Simulated results of port 2.

observed from Fig.11 that the isolation of |S21| and |S23| between adjacent antennas has been increased by 10.8 (from 12.1 to 22.9 dB) and 17.5 dB (from 13.1 to 30.6 dB) respectively. The isolation of |S31| enhances by 16.6 dB (from 17.5 to 34.1 dB). Moreover, the 10-dB impedance bandwidth of antenna 2 increases by 86 MHz (from 114 MHz to 200 MHz). It is also seen that the mutual coupling of the array is less −20 dB within the 10-dB impedance bandwidth of the antenna, demonstrating the potential for a wide band decoupling.

B. RADIATION PROPERTIES

Fig.12 shows the simulated and measured radiation patterns for xoz-plane and yoz-plane at various operational frequencies of 3.95 GHz, 4 GHz and 4.05 GHz. After loading the decoupling structure, the radiation pattern of the antenna is basically unchanged, expect that the level of the back lobe is slightly increased on the yoz-plane. The comparison in Fig.12 shows that, within the 10-dB impedance bandwidth, no distortion occurs in the radiation pattern of the antenna after the decoupling structure is loaded. In addition, the measured results do not match the simulated results perfectly, which may be attributed to the measurement and manufacturing errors.

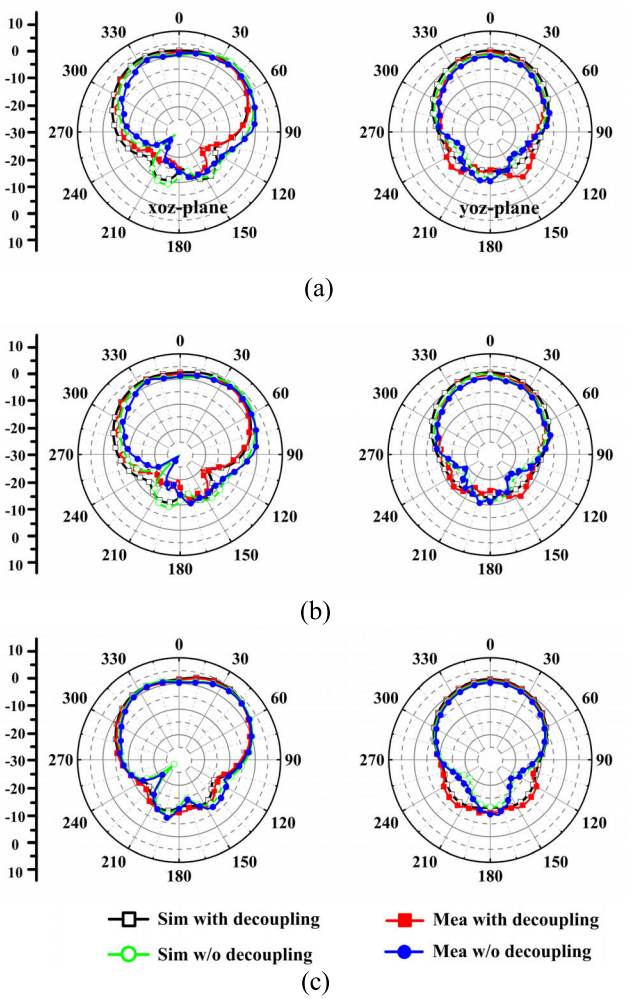

FIGURE 12. Simulated and measured radiation patterns (in realized gain) of the three-element array with and without the decoupling structure. (the antenna 1 is excited and antenna 2 and 3 are terminated with 50 Ω). (a) 3.95 GHz. (b) 4 GHz. (c) 4.05 GHz.

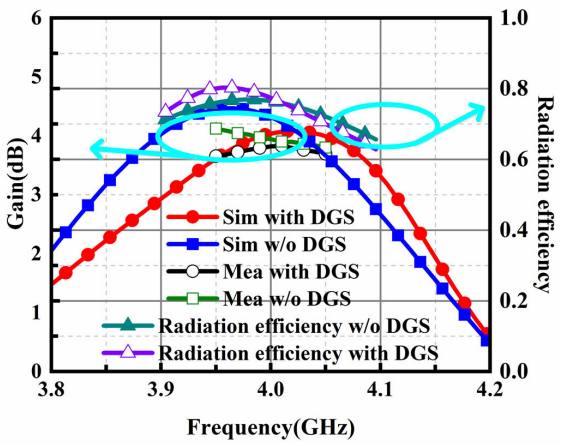

FIGURE 13. Simulated and measured gain with and without the decoupling structure.

The gain and radiation efficiency of the antenna is shown in Fig.13. According to the measurement results, the gain at the center frequency slightly decreases (from 3.94 to 3.82 dB)

TABLE 2. Comparision of the proposed decoupling structure and other decoupling technique.

Paper	Frequency (GHz)	Decoupling Structures	Substrate	Complexity	Antenna Type	Edge-to-Edge Spacing	Enhancement in |S21|, |S31| and |S23| (dB)
[7]	5.8	Polarization conversion isolator	N/A	Yes	1×2	0.18 λ_0	19.6
[13]	3.5	Parallel coupled-line resonators	FR4	No	1×2	0.07 λ_0	26.2
[22]	2.45	ADS	F4B	No	1×8	0.081 λ_0	avenge 15
[32]	5.8	Interdigital lines	Rogers RO4003	No	1×3	0.07 λ_0	30, 8.5, N/A
[33]	3.325	Capacitively loaded loop	N/A	Yes	1×2	0.12 λ_0	55
[34]	2.45	Waveguided metamaterials	Taconic	Yes	1×2	0.093 λ_0	18
[35]	4.8	DGS	Rogers RO3003	No	1×2	0.05 λ_0	26
[36]	5	Resonators	N/A	Yes	1×2	0.25 λ_0	10
[37]	10	EBG	FR4	No	1×3	0.33 λ_0	avenge 30
[38]	8.85	EBG	FR4	Yes	2×2	0.5 λ_0	17, 37, N/A
[39]	10	Matamaterial	FR4	No	1×2	0.66 λ_0	avenge 11
This	4	DGS with metal vias	FR4	No	1×3	0.037 λ_0	10.8, 16.6, 17.5

after the decoupling structure is loaded. The radiation efficiency of the antenna array without and with the decoupling structure is 76.2% and 76.7% respectively at 4 GHz. It proves that the decoupling structure has little effect on the radiation efficiency.

V. CONCLUSION

The T-shaped and rectangular ring structure with six metal-vias is shown to be an effective tool for attenuating the ground coupling current in the 1 × 3 E-plane patch antenna array at 4 GHz. One important advantage of the decoupling structure is that it can improve isolation in tightly spaced (0.037 λ_0) linear array. From the comparison with other designs in employing artificial structures for decoupling patches in TABLE 2, it can be summarized that the proposed decoupling structure achieved the isolation of better 20 dB with the smallest edge separations. Moreover, the bandwidth of antenna 2 is increased by 86 MHz under the effect of the structure. The measured results show that the novel decoupling structure can be applied to linear antenna array.

REFERENCES

[1] X. Li, L. Yang, and L. Huang, "Novel design of 2.45-GHz rectenna element and array for wireless power transmission," *IEEE Access*, vol. 7, pp. 28356–28362, 2019.

[2] Q. Chen and H. Zhang, "High-gain circularly polarized Fabry–Pérot patch array antenna with wideband low-radar-cross-section property," *IEEE Access*, vol. 7, pp. 8885–8889, 2019.

[3] M. Sonkki, D. Pfeil, V. Hovinen, and K. R. Dandekar, "Wideband planar four-element linear antenna array," *IEEE Antennas Wireless Propag. Lett.*, vol. 13, pp. 1663–1666, 2014.

[4] J. L. Allen and B. L. Diamond, "Mutual coupling in array antennas," MIT Lincoln Lab., Lexington, MA, USA, Tech. Rep. 424 (ESD-TR-66-443), 1966.

[5] F. Liu, J. Guo, L. Zhao, X. Shen, and Y. Yin, "A meta-surface decoupling method for two linear polarized antenna array in sub-6 GHz base station applications," *IEEE Access*, vol. 7, pp. 2759–2768, 2018.

[6] Z. Wang, L. Zhao, Y. Cai, S. Zheng, and Y. Yin, "A meta-surface antenna array decoupling (MAAD) method for mutual coupling reduction in a MIMO antenna system," *Sci. Rep.*, vol. 8, no. 1, 2018, Art. no. 3152.

[7] Y.-F. Cheng, X. Ding, W. Shao, and B.-Z. Wang, "Reduction of mutual coupling between patch antennas using a polarization-conversion isolator," *IEEE Antennas Wireless Propag. Lett.*, vol. 16, pp. 1257–1260, 2016.

[8] M. Alibakhshikenari, M. Khalily, B. S. Virdee, C. H. See, R. Abd-Alhameed, and E. Limiti, "Mutual coupling suppression between two closely placed microstrip patches using EM-bandgap metamaterial fractal loading," *IEEE Access*, vol. 7, pp. 23606–23614, 2019.

[9] M. Alibakhshikenari, M. Khalily, B. S. Virdee, C. H. See, R. A. Abd-Alhameed, and E. Limiti, "Mutual-coupling isolation using embedded metamaterial EM bandgap decoupling slab for densely packed array antennas," *IEEE Access*, vol. 7, pp. 51827–51840, 2019.

[10] X. Yang, Y. Liu, Y.-X. Xu, and S.-X. Gong, "Isolation enhancement in patch antenna array with fractal UC-EBG structure and cross slot," *IEEE Antennas Wireless Propag. Lett.*, vol. 16, pp. 2175–2178, 2017.

[11] X. Tan, W. Wang, Y. Wu, Y. Liu, and A. A. Kishk, "Enhancing isolation in dual-band meander-line multiple antenna by employing split EBG structure," *IEEE Trans. Antennas Propag.*, vol. 67, no. 4, pp. 2769–2774, Apr. 2019.

[12] B. L. Dhevi, K. S. Vishvaksenan, and K. Rajakani, "Isolation enhancement in dual-band microstrip antenna array using asymmetric loop resonator," *IEEE Antennas Wireless Propag. Lett.*, vol. 17, no. 2, pp. 238–241, Feb. 2018.

[13] K. S. Vishvaksenan, K. Mithra, R. Kalaiarasan, and K. S. Raj, "Mutual coupling reduction in microstrip patch antenna arrays using parallel coupled-line resonators," *IEEE Antennas Wireless Propag. Lett.*, vol. 16, pp. 2146–2149, 2017.

[14] A. Diallo, C. Luxey, P. Le Thuc, R. Staraj, and G. Kossiavas, "Study and reduction of the mutual coupling between two mobile phone PIFAs operating in the DCS1800 and UMTS bands," *IEEE Trans. Antennas Propag.*, vol. 54, no. 11, pp. 3063–3074, Nov. 2006.

[15] Y. Wang and Z. Du, "A wideband printed dual-antenna with three neutralization lines for mobile terminals," *IEEE Trans. Antennas Propag.*, vol. 62, no. 3, pp. 1495–1500, Mar. 2014.

[16] S.-W. Su, C.-T. Lee, and F.-S. Chang, "Printed MIMO-antenna system using neutralization-line technique for wireless USB-dongle applications," *IEEE Trans. Antennas Propag.*, vol. 60, no. 2, pp. 456–463, Feb. 2012.

[17] S. Wang and Z. Du, "Decoupled dual-antenna system using crossed neutralization lines for LTE/WWAN smartphone applications," *IEEE Antennas Wireless Propag. Lett.*, vol. 14, pp. 523–526, 2014.

[18] J. C. Coetzee and Y. Yu, "Port decoupling for small arrays by means of an eigenmode feed network," *IEEE Trans. Antennas Propag.*, vol. 56, no. 6, pp. 1587–1593, Jun. 2008.

[19] X. Tang, X. M. Qing, and Z. N. Chen, "Simplification and implementation of decoupling and matching network with port pattern-shaping capability for two closely spaced antennas," *IEEE Trans. Antennas Propagation.*, vol. 63, no. 8, pp. 3695–3699, Aug. 2015.

[20] X. Tang, K. Mouthaan, and J. C. Coetzee, "Tunable decoupling and matching network for diversity enhancement of closely spaced antennas," *IEEE Antennas Wireless Propag. Lett.*, vol. 11, pp. 268–271, 2012.

[21] M. Li, B. G. Zhong, and S. W. Cheung, "Isolation enhancement for MIMO patch antennas using near-field resonators as coupling-mode transducers," *IEEE Trans. Antennas Propag.*, vol. 67, no. 2, pp. 755–764, Feb. 2019.

[22] K.-L. Wu, C. Wei, X. Mei, and Z.-Y. Zhang, "Array-antenna decoupling surface," *IEEE Trans. Antennas Propag.*, vol. 65, no. 12, pp. 6728–6738, Dec. 2017.

[23] B. Zhang, J. M. Jornet, I. F. Akyildiz, and Z. P. Wu, "Mutual coupling reduction for ultra-dense multi-band plasmonic nano-antenna arrays using graphene-based frequency selective surface," *IEEE Access*, vol. 7, pp. 33214–33225, 2019.

[24] X. Zou, G.-M. Wang, and Y. Wang, "Microstrip antenna array of connected elements using X-shaped connection line," *IEEE Antennas Wireless Propag. Lett.*, vol. 17, no. 5, pp. 890–893, May 2018.

[25] X.-J. Zou, G.-M. Wang, Y.-W. Wang, and H.-P. Li, "An efficient decoupling network between feeding points for multielement linear arrays," *IEEE Trans. Antennas Propag.*, vol. 67, no. 5, pp. 3101–3108, May 2019.

[26] L. Wang, Z. Xing, K. Wei, R. Xu, and J. Li, "S-shaped periodic defected ground structures to reduce microstrip antenna array mutual coupling," *Electron. Lett.*, vol. 52, no. 15, pp. 1288–1290, Jul. 2016.

[27] M. S. Sharawi, A. B. Numan, M. U. Khan, and D. N. Aloi, "A dual-element dual-band MIMO antenna system with enhanced isolation for mobile terminals," *IEEE Antennas Wireless Propag. Lett.*, vol. 11, pp. 1006–1009, 2012.

[28] J. Y. Deng, J. Li, L. Zhao, and L. Guo, "A dual-band inverted-F MIMO antenna with enhanced isolation for WLAN applications," *IEEE Antennas Wireless Propag. Lett.*, vol. 16, pp. 2270–2273, 2017.

[29] K. Wei, J.-Y. Li, L. Wang, and R. Xu, "Microstrip antenna array mutual coupling suppression using coupled polarisation transformer," *IET Microw., Antennas Propag.*, vol. 11, no. 13, pp. 1836–1840, Oct. 2017.

[30] Z. Niu, H. Zhang, Q. Chen, and T. Zhong, "A novel defect ground structure for decoupling closely spaced E-plane microstrip antenna array," *Int. J. Microw. Wireless Technol.*, pp. 1–6, May 2019.

[31] A. Ghalib and M. S. Sharawi, "TCM analysis of defected ground structures for MIMO antenna designs in mobile terminals," *IEEE Access*, vol. 5, pp. 19680–19692, 2017.

[32] H. Qi, X. Yin, L. Liu, Y. Rong, and H. Qian, "Improving isolation between closely spaced patch antennas using interdigital lines," *IEEE Antennas Wireless Propag. Lett.*, vol. 15, pp. 286–289, 2016.

[33] A. Jafargholi, A. Jafargholi, and H. Jun Choi, "Mutual coupling reduction in an array of patch antennas using CLL metamaterial superstrate for MIMO applications," *IEEE Trans. Antennas Propag.*, vol. 67, no. 1, pp. 179–189, Jan. 2019.

[34] Z. Qamar and H. C. Park, "Compact waveguided metamaterials for suppression of mutual coupling in microstrip array," *Progr. Electromagn. Res.*, vol. 149, pp. 183–192, 2014.

[35] A. I. Hammoodi, A. A. Isaac, and H. Raad, "Isolation enhancement between two closely spaced circular patches using DGS," in *Proc. IEEE Int. Symp. Antennas Propag. USNC/URSI Nat. Radio Sci. Meeting*, Jul. 2017, pp. 2273–2274.

[36] M. M. Bait-Suwailam, O. F. Siddiqui, and O. M. Ramahi, "Mutual coupling reduction between microstrip patch antennas using slotted-complementary split-ring resonators," *IEEE Antennas Wireless Propag. Lett.*, vol. 9, pp. 876–878, 2010.

[37] M. Alibakhshikenari, M. Vittori, S. Colangeli, B. S. Virdee, A. Andújar, J. Anguera, and E. Limiti, "EM isolation enhancement based on metamaterial concept in antenna array system to support full-duplex application," in *Proc. IEEE Asia Pacific Microw. Conf. (APMC)*, Nov. 2017, pp. 740–742.

[38] M. Alibakhshikenari, B. S. Virdee, C. H. See, R. Abd-Alhameed, A. H. Ali, F. Falcone, and E. Limiti, "Study on isolation improvement between closely-packed patch antenna arrays based on fractal metamaterial electromagnetic bandgap structures," *IET Microw. Antennas Propag.*, vol. 12, no. 14, pp. 2241–2247, Nov. 2018.

[39] M. Alibakhshikenari, B. S. Virdee, P. Shukla, C. H. See, R. Abd-Alhameed, M. Khalily, F. Falcone, and E. Limiti, "Interaction between closely packed array antenna elements using meta-surface for applications such as mimo systems and synthetic aperture radars," *Radio Sci.*, vol. 53, no. 11, pp. 1368–1381, Nov. 2018.

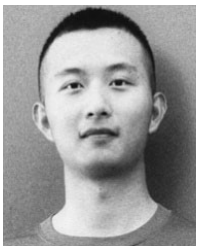

ZICHENG NIU was born in Hebei, China, in 1996. He received the bachelor's degree from the Nanjing University of Posts and Telecommunications (NJUPT), Nanjing, China, in 2017. He is currently pursuing the master's degree in electrical science and technology with Air Force Engineering University (AFEU), Xi'an, China. His research interests include MIMO antenna and array decoupling.

HOU ZHANG received the B.S. degree from Xi'an Electronic and Engineering University, the M.S. degree from Air Force Missile College, and the Ph.D. degree from Xidian University, all in electromagnetic field and microwave technology. He has published over 150 technical articles and authored/edited six books. He holds six granted/filed patents. He is currently interested in planar antennas and EMC. He has been the Session Chair of PIERS and APEMC.

QIANG CHEN was born in Jiangxi, China. He received the B.S., M.S., and Ph.D. degrees from Air Force Engineering University (AFEU), Xi'an, China, in 2011, 2013, and 2019, respectively. His research interests include microwave circuits, antennas, and arrays.

TAO ZHONG was born in Hubei, China. He received the M.S. degree in electromagnetic field and microwave technology from Air Force Engineering University (AFEU), Xi'an, China, in 2016, where he is currently pursuing the Ph.D. degree in electrical science and technology. His research interests include leaky-wave antennas, transmission line, and array antennas.